Acoustic attenuation in gas mixtures with nitrogen: Experimental data and calculations

Sally G. Ejakov[a)]
Center for Sensor Materials, Michigan State University, East Lansing, Michigan 48824-1116

Scott Phillips
Commercial Electronics, Broken Arrow, Oklahoma 74012-2838

Yefim Dain and Richard M. Lueptow[b)]
Department of Mechanical Engineering, Northwestern University, Evanston, Illinois 60208-3111

Jacobus H. Visser
Ford Research Laboratory, Mail Drop 3083/Scientific Research Laboratory, Dearborn, Michigan 48121-2053

(Received 31 July 2002; revised 20 December 2002; accepted 13 January 2003)

Attenuation in a gas results from a combination of classical attenuation, attenuation from diffusion, and attenuation due to molecular relaxation. In previous papers [J. Acoust. Soc. Am. **109**, 1955 (2001); **110**, 2974 (2001)] a model is described that predicts the attenuation from vibrational relaxation in gas mixtures. In order to validate this model, the attenuation was measured using a pulse technique with four transducer pairs, each with a different resonant frequency. The attenuation calculated using the model was compared to the measured values for a variety of gases including: air, oxygen, methane, hydrogen, and mixtures of oxygen/nitrogen, methane/nitrogen, carbon dioxide/nitrogen, and hydrogen/nitrogen. After the measured data is corrected for diffraction, the model matches the trends in the measured attenuation spectrum for this extensive set of gas mixtures. © *2003 Acoustical Society of America.* [DOI: 10.1121/1.1559177]

PACS numbers: 43.35.Ae [RR]

I. INTRODUCTION

Attenuation in gases results from several mechanisms that transfer the translational energy of the acoustic wave into other forms of energy. These mechanisms include classical effects related to viscosity and thermal conductivity, losses due to diffusion in gas mixtures, and losses due to excitation and relaxation of vibrational or rotational molecular energy levels in the gas.[1] Classical acoustic attenuation results from irreversible losses of acoustic energy to heat due to shear viscosity and thermal conductivity across temperature gradients related to the compression and rarefaction of the acoustic wave. Classical attenuation is well understood and can be predicted for ideal gases, both pure and in mixtures, as long as the viscosity and conductivity of the mixture are known. Attenuation due to diffusion occurs in mixtures when light gas molecules diffuse faster than heavier ones locally changing the mixture composition as the acoustic wave passes. This loss of entropy in the arrangement of molecules results in a reduction in the energy in the acoustic wave. Attenuation related to diffusion is largest for mixtures of gases having much different masses (e.g., hydrogen/nitrogen mixtures). The attenuation from diffusion can be calculated for gas mixtures, if the appropriate constants are known.[2] Exciting the energy states of the gas molecules and the relaxation of these states also causes attenuation. The transfer of translational energy to internal modes occurs with a relaxation time that depends on the collisional dynamics of the internal vibrational modes available and is different than the time required to equilibrate the translational energy. The collisional dynamics in some gases result in relaxation times that correspond to relaxation frequencies ranging from a few Hz up to 10 MHz, where a significant increase in attenuation can be observed. On the other hand, rotational modes in the molecules typically have much shorter relaxation times and consequently usually affect the attenuation only at much higher frequencies.

The relaxation of vibrational modes in a molecule results in attenuation that is strongly dependent on the gases present. In gas mixtures with more than two species, the interactions of vibrational modes and their effect on attenuation were not fully quantified until recently. To remedy this, two of us, Dain and Lueptow, developed a model that describes molecular relaxation for mixtures of gases.[3,4] In brief, this model numerically solves the Euler gas equations and the population equations for the energy states of the molecules (including collision rates and transition probabilities).[5–7] More details of the calculations in particular as they apply to the molecular species reported in this paper are given in the Appendix. The calculations agree well with measurements reported in the literature for the cases where they can be compared.[3] Unfortunately, the available measurements of attenuation in gases cover only limited species, report many results only at elevated temperatures, and contain some discrepancies even for single component gases.[8–13] This study is focused on measurements of the at-

[a)]Current address: Ford Motor Company, POEE Mail Drop 43, 21500 Oakwood Boulevard, Dearborn, MI 48124; electronic mail: gaffsall@msu.edu
[b)]Email: r-lueptow@northwestern.edu

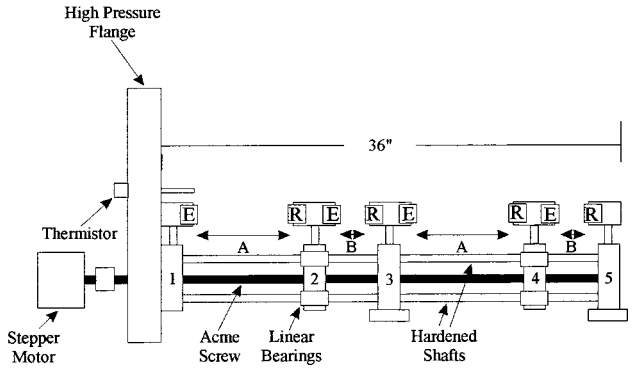

FIG. 1. A schematic diagram of the transducer traverse system mounted on the high-pressure flange. The stepper motor moves supports 2 and 4. This whole assembly was sealed inside a cylindrical chamber.

tenuation at room temperature for several binary mixtures of practical interest including methane/nitrogen, carbon dioxide/nitrogen, oxygen/nitrogen, and hydrogen/nitrogen mixtures. Our objective in this research was twofold. First we used an experimental apparatus similar to that used previously,[14] but incorporating modern transducers and electronics technology, to accurately measure acoustic attenuation in gas mixtures. Second, we compare our experimental results with previous results and our model results to further validate our model.

II. EXPERIMENTAL DESCRIPTION

Measurements of the attenuation in various gases were carried out in a large cylindrical chamber with a diameter of 30.5 cm (12 inches) and a length of 91.5 cm (36 inches). Figure 1 shows the transducer traverse system mounted on the high-pressure flange that seals one end of the chamber. The supports (labeled 1–5) hold four sets of transducers, with supports 2, 3, and 4 each holding both an emitter (E) and a receiver (R). The acoustic measurements are made between an emitter on one support, for example, support 1, and a receiver on the next support, in this case support 2, with a separation distance A between the transducers. A stepper motor drives an Acme screw to displace supports 2 and 4 with a resolution of 0.001 cm (0.0005 inches) per step, while the other supports (1, 3, and 5) remain stationary. The transducer positions are zeroed at the beginning of each test, and the separation between transducers is measured to within 0.003 cm (0.001 inches). In these measurements the distance between the emitter and receiver of each pair was adjusted from 0.762 to 19.812 cm (0.300–7.800 inches) using 75 steps.

At the beginning of each test, the chamber was evacuated to 0.0003 atm (0.05 psi), filled to 0.7 atm (10 psi) with the test gas, evacuated again to 0.0003 atm and then filled to a high pressure (30 atm) with a precise mixture of gases. The gas mixing for the chamber was controlled with mass flow controllers and a specially designed regulator that allows the test chamber to be pressurized, while the output pressure for the mass flow controllers was held constant providing the gas composition to within 0.01%. The nitrogen, air, oxygen, methane, carbon dioxide, and hydrogen used in these tests were all 99.99 or 99.999% pure.

Since attenuation depends on frequency divided by pressure (f/p), either frequency or pressure can be varied. Because the transducers are tuned to a particular resonant frequency, it is easier and more effective to vary the pressure in the chamber than to vary the transducer frequency. Thus, measurements of the attenuation were made at the initial high gas pressure, and then some gas was removed from the chamber and the test performed again. Measurements were made at 11 different pressures from 30–0.6 atm.

Four sets of transducers were used in a pitch–catch configuration. The piezoelectric transducer pairs had matched frequencies of 92 kHz, 149.1 kHz, 215 kHz, and 1 MHz. Other details of the transducers are listed in Table I. After the gas filled the chamber to the correct pressure and the transducers had been moved to the appropriate separation distances using the stepper motor, the first emitter was excited with a burst of 10 pulses at the frequency of the transducer pair. (Bursts of 1 and 5 pulses give similar values for attenuation, but the amplitude is smaller, so 10 pulses were preferred.) Accounting for the speed of sound in the gas mixture being tested, the signal that corresponded to the original pulse measured at the receiver was recorded. In addition, the pressure and temperature in the test chamber along with other parameters were recorded. Each emitter was energized individually and after all four emitters had been pulsed, the

TABLE I. Data related to the transducers, including: transducer radius (R), transition point (R^2/λ), and the fit region used in the analysis for the individual gases for each transducer pair.

Frequency (kHz)	R (cm)	R^2/λ (cm) air	Fit region (cm) air	R^2/λ (cm) O_2	Fit region (cm) O_2	R^2/λ (cm) CH_4	Fit region (cm) CH_4	R^2/λ (cm) CO_2	Fit region (cm) CO_2	R^2/λ (cm) H_2	Fit region (cm) H_2
92[a]	1.3	4.52	12.700–19.812	4.42	12.700–19.812	3.49	12.700–19.812	5.56	7.620–12.700	1.20	12.700–19.812
149.1[b]	0.9	3.51	7.620–19.812	3.43	7.620–19.812	2.71	7.620–19.812	4.32	7.620–12.700	0.93	7.620–19.812
215[a]	0.6	2.25	7.620–19.812	2.20	7.620–19.812	1.74	7.620–19.812	2.77	7.620–12.700	0.59	7.620–19.812
1000[b]	1.0	29.07	0.762–7.620	28.42	0.762–7.620	22.44	0.760–7.620	35.74	0.760–2.540	7.69	0.762–7.620

[a]Manufactured by ITC.
[b]Manufactured by Etalon.

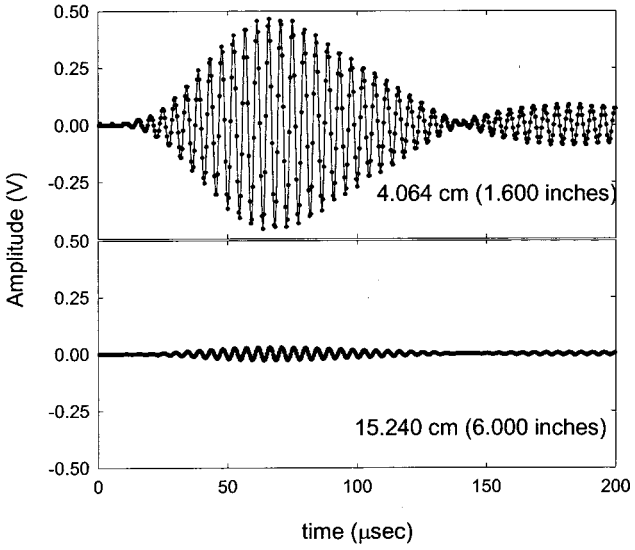

FIG. 2. Raw signals from the 215 kHz transducer in 100% methane at a chamber pressure of 3.18 atm at two different separation distances, 4.064 cm and 15.240 cm.

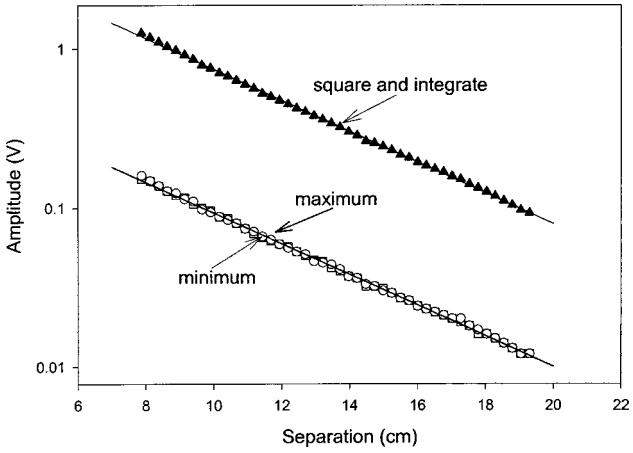

FIG. 3. Amplitude vs separation distance for 100% methane, the 215 kHz transducers, and a pressure of 3.18 atm. The amplitude was evaluated as the maximum or largest value of the data set (squares), the minimum or absolute value of the most negative value in the data set (circles), and the sum of each point in the data set squared (triangles). The curves are least-squares fits to the data.

transducers were moved to a new separation distance and the measurement was repeated. When the range of separation distances had been covered, the pressure was reduced for the next set of tests, and the test protocol was repeated.

Measurements were made in several gases, both pure gases (oxygen, methane, and hydrogen) and mixtures (air, oxygen/nitrogen, methane/nitrogen, carbon dioxide/nitrogen, and hydrogen/nitrogen). (Pure carbon dioxide has such a strong attenuation that the resulting pulses at the receiver were below our detection threshold, so data could not be obtained in this case.) The mixtures were tested in concentration steps of 20% from 20–80%. The chamber was at ambient temperature, with an average temperature during a test between 292.6 and 298.6 K. While this temperature range is relatively small, it affects the attenuation to some extent. Using our model of attenuation, we estimate that the attenuation can change by a maximum of 10% over this temperature range, depending on the gases present. However, the temperature range for any given test was smaller, varying by 1.0–3.5 K.

III. DATA ANALYSIS

The harmonic acoustic pressure P decreases with distance z from the emitter according to

$$P = P_0 e^{-\alpha z}, \tag{1}$$

where P_0 is the amplitude of the acoustic pressure at the emitter, and α is the attenuation. In our tests the voltage produced in the receiving transducer by the sound wave is proportional to the acoustic pressure. Therefore, the attenuation can be found from the slope of the logarithm of the voltage amplitude plotted as a function of separation distance according to Eq. (1). This equation is exact for plane waves, but requires a correction for diffraction of a sound wave emitted from a transducer of finite size, discussed shortly.

For each gas mixture, transducer pair, and separation distance, the raw data consists of the receiver voltage versus time, as shown in Fig. 2 for the 215 kHz transducer with 100% methane at a pressure of 3.18 atm (46.76 psi). The entire data set of 512 points was recorded over 40 μs for the 1 MHz transducer, 200 μs for the 149.1 and 215 kHz transducers, and 400 μs for the 92 kHz transducer. The form of the wave packet is typical of the transducer response and does not show the first reflection, which arrived 182 μs after the original wave for the 4.064 cm separation distance. Even though the emitter was excited with only 10 pulses, ringing of the emitter results in two to three times that number of peaks in the voltage being recorded at the receiver. (The second series of pulses at about 150 μs are anomalous signals possibly related to transducer ringing or reflections from the mounting system. They were omitted from the analysis.) The decrease in amplitude resulting from attenuation as the separation distance is increased from 4.064 to 15.240 cm is evident in Fig. 2.

Three methods were evaluated to measure the amplitude of the signal at the receiver: the maximum of the signal (largest value observed), the minimum of the signal (absolute value of the most negative value observed), and the integral of the square of the signal, which is equivalent to the sound intensity. No curve fitting was used for the maximum and minimum as the raw data has enough resolution to provide points very close to the extrema. For all three methods to evaluate the amplitude, the log of the voltage amplitude (which is proportional to acoustic pressure) plotted as a function of separation distance should yield a linear relationship with a slope of α, in accordance with Eq. (1). Figure 3 compares the amplitude of the signal evaluated using the three methods as a function of separation distance for a typical data set. Although the magnitude of the amplitude depends on the method of evaluation, the slope, which corresponds to the attenuation α, is very similar for all three techniques. Consequently, the maximum of the signal was used to determine the attenuation, since it is most convenient and provides identical results as shown in Fig. 3.

In order to accurately determine the physical attenua-

tion, it is necessary to correct for any other effects that also change the amplitude of the acoustic wave with separation distance such as spreading and diffraction. The sound field has many maxima and minima that approximately average out in the near field region close to the emitting transducer so that no correction is needed. However, a correction is needed in the far field as the sound decreases in amplitude due to spreading and diffraction as the distance from the emitter increases.[15] It is important to measure the attenuation either completely in the near field or completely in the far field to avoid difficulty in accounting for the diffraction.[16] The transition between these two regions occurs at approximately R^2/λ, where R is the transducer radius and λ is the wavelength of the sound.[17] The values for this transition point for each transducer pair evaluated for pure gases used in these measurements are given in Table I. In many cases, the transition between the near and far fields occurs within the range of separation distances (0.762–19.812 cm) in our experiments.

For each gas composition and transducer pair it is necessary to choose the range of separation distances corresponding to either the far or near field that should be used to find the attenuation, α. The ranges that were used are shown in Table I for the pure gases. Mixtures of these gases with nitrogen were analyzed over the range used for the pure gas. The data measured in the far field was used for the three lower frequency transducers. For the 1 MHz transducer the data in the near field was used, but the range of data was further restricted to separation distances less than 7.620 cm, because at larger separation distances the strong attenuation at this frequency reduced the signal to such a low amplitude that it was no longer measurable. Because carbon dioxide has greater attenuation than the other gases, the maximum separation was further restricted in these cases.

For the three lower frequency transducers, it is necessary to correct the data for diffraction in the far field. We considered two diffraction correction methods. Pinkerton calculated the amplitude, $A(z)$, on the axis of the coaxial transducers as

$$A(z)=A_0 e^{-\alpha z}\{\sin[\tfrac{1}{2}k(\{z^2+R^2\}^{1/2}-z)]\}, \tag{2}$$

where A_0 is the amplitude at the emitter, $k=2\pi/\lambda$ is the wave number, and z is the separation between the emitter and the receiver.[16] A more precise diffraction correction was developed by Khimunin[18] for harmonic waves based on Williams' formula for average pressure on a receiver.[19] Rogers and Van Buren used a simplified version of this expression integrating the acoustic amplitude over the surface of the emitter and the receiver, both of radius R, to find a short wave approximation ($ka \gg 1$) for the total average amplitude

$$A(z)=A_0 e^{-\alpha z}\left\{\left[\cos\left(\frac{2\pi}{s}\right)-J_0\left(\frac{2\pi}{s}\right)\right]^2+\left[\sin\left(\frac{2\pi}{s}\right)-J_1\left(\frac{2\pi}{s}\right)\right]^2\right\}^{1/2}, \tag{3}$$

where $s=2\pi z/kR^2$, J_0 and J_1 are zero and first order Bessel functions, and z is the separation between the transducers.[20] Both of these corrections assume that diffraction and attenuation are independent processes. The exponential is related to the attenuation, while the term in brackets is the diffraction correction. Ideally, a complex wave number should be used in Eqs. (2) and (3) to incorporate the effect of acoustic attenuation on diffraction. In addition, Eqs. (2) and (3) were developed for harmonic waves but not for bursts, which were used in these experiments. Nevertheless, both methods provided good results. An analysis incorporating a complex wave number (and thereby attenuation) into a diffraction correction for bursts rather than harmonic waves in a relaxing medium will be addressed in a separate paper.[21]

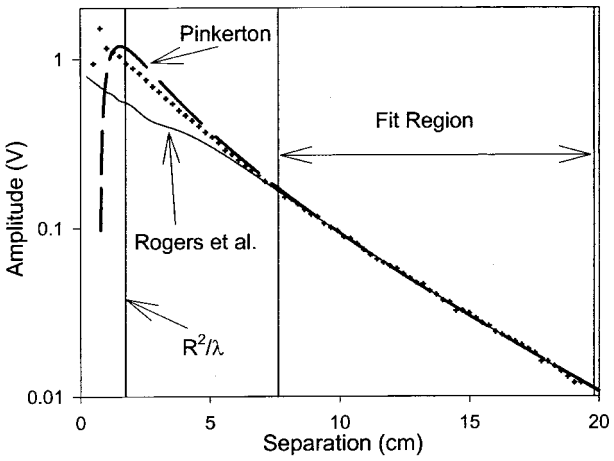

FIG. 4. Amplitude of the sound wave as a function of separation distance for 100% methane, the 215 kHz transducers and 3.18 atm. The dots show the measurements. The diffraction correction method of Pinkerton [Eq. (2)], $\alpha=0.375$, is the dashed curve, and the diffraction correction method of Rogers *et al.* [Eq. (3)], $\alpha=0.397$, is the solid curve.

The two diffraction corrections are compared with the raw data in Fig. 4 for tests of 100% methane using the 215 kHz transducer. In both cases, the attenuation α in Eqs. (2) and (3) was adjusted to provide the best fit with the data in the fit region noted in Table I. In the fit region both corrections match the data well, but at shorter separation distances, near the transition between the near and far field, the simpler Pinkerton form follows the data better. This result was confirmed by calculating the attenuation for all of the chamber pressures and transducers for the gas mixtures measured. The diffraction correction was applied by dividing the intensity at each separation distance by the calculated correction at that distance and then fitting the resulting curve to find α. Applying the Pinkerton correction to the data in the standard attenuation spectrum form of $\alpha\lambda$ as a function of f/p results in an overlap between the data from different transducers at the same f/p (as will be evident in Figs. 5–12, which will be discussed later). The Rogers and Van Buren correction does not result in overlap of the data for the different transducers when plotted as an attenuation spectrum, even when the radius R in Eq. (3) is replaced by an effective radius that is some fraction of R. Thus, the Pinkerton correction for diffraction was used for all of the data that is presented in the next section.

IV. RESULTS

In this section we present the results of attenuation measurements for several pure gases and gas mixtures, most of

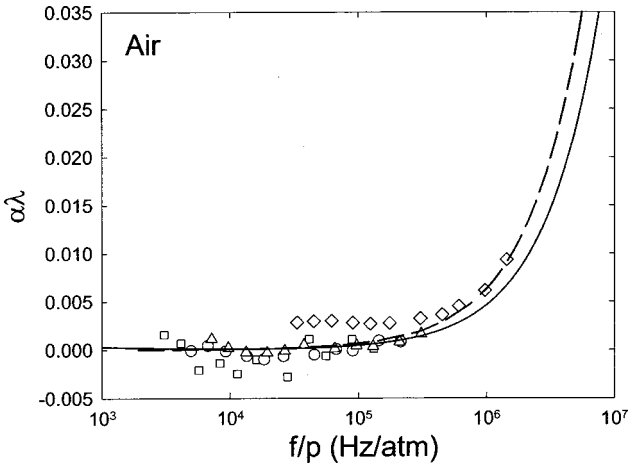

FIG. 5. Results for air using the Pinkerton diffraction correction at an average temperature of 293.1 K. Data points are for the 92 kHz, 149.1 kHz, 215 kHz, and 1 MHz transducers (squares, circles, triangles, and diamonds, respectively). The solid curve is the classical attenuation and the dashed curve is the empirical model from Bass *et al.* (Ref. 1).

which have not been previously measured. These results are useful in understanding the effect of gas composition on acoustic attenuation. In addition, we compare the experimental results with the sum of the theoretical model of Dain and Lueptow[3] for vibrational relaxation, the classical attenuation, and the diffusional attenuation. This allows us to determine the effectiveness of the vibrational relaxation model in predicting acoustic attenuation. The classical attenuation was calculated using the Stokes and Kirchoff formulation, and the attenuation due to diffusion was calculated from Bhatia's formulations.[2] More details on the vibrational relaxation calculations are included in the Appendix. In all cases we plot the attenuation α nondimensionalized by the wavelength λ as a function of the frequency divided by the pressure, f/p, which can be called an attenuation spectrum.

A. Air

The acoustic attenuation spectrum for air is shown in Fig. 5. It is immediately evident that the different transducers

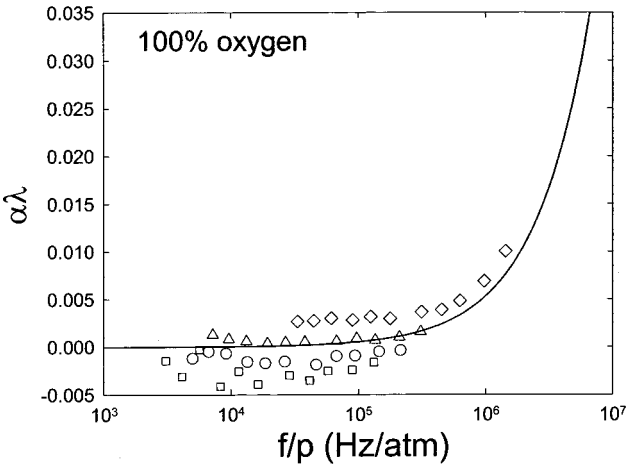

FIG. 6. Results for 100% oxygen using the Pinkerton diffraction correction at an average temperature of 293.3 K. Data points are for the 92 kHz, 149.1 kHz, 215 kHz, and 1 MHz transducers (squares, circles, triangles, and diamonds, respectively). The solid curve is the classical attenuation. Vibrational relaxation is negligible.

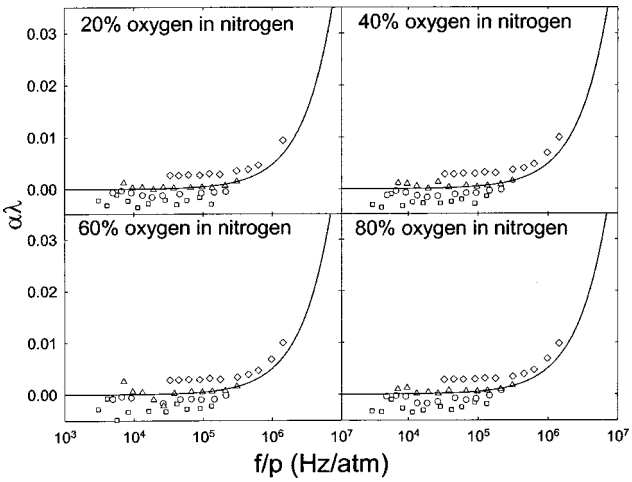

FIG. 7. Results for mixtures of 20%, 40%, 60%, and 80% oxygen in nitrogen using the Pinkerton diffraction correction at average temperatures of 293.6, 292.8, 292.8, and 293.9 K, respectively. Data points are for the 92 kHz, 149.1 kHz, 215 kHz, and 1 MHz transducers (squares, circles, triangles, and diamonds, respectively). The solid curves are the sum of the classical and diffusional attenuation. Vibrational relaxation is negligible.

having frequencies of 92 kHz to 1 MHz (indicated by different symbols) give similar values. The values from the 1 MHz transducer (diamonds) are slightly higher, possibly because the results are based on measurements in the near field rather than in the far field, as with the other transducers. Nevertheless, the agreement between results from transducers differing by an order of magnitude in frequency indicates that the experimental apparatus and procedure are robust. Many previous experiments in air have been used to develop an empirical formula for the acoustic attenuation in air at a variety of temperatures and humidities.[1] The empirical model accounts for classical attenuation and attenuation from relaxation of vibrational and rotational modes. The curves in Fig. 5 indicate both the classical component only (solid curve) and the full form of the empirical fit for air (dashed curve). The difference between these curves comes primarily from the relaxation of rotational modes in the air. The increase in $\alpha\lambda$ at higher frequencies agrees well with the classical model, although the empirical model fits the data even better. The negative attenuation evident at lower frequencies arises from the diffraction correction and the error in the experiments. Comparable anomalous negative attenuation has occurred previously in similar measurements.[22] Even so, the empirical model matches the data quite well.

B. Oxygen

Pure oxygen and mixtures of oxygen and nitrogen were also tested. Figure 6 shows the data for pure oxygen, while Fig. 7 shows the results for various mixtures of oxygen and nitrogen. The relaxation frequency of oxygen has been found to be at about 3 Hz at atmospheric pressure,[23] which is below our measurement capability. Our data agrees well with the classical calculations indicated by the curves in the figures. These plots provide more evidence of the reliability of the experimental technique. The model calculations from Dain and Lueptow[3] are consistent with the observation that the

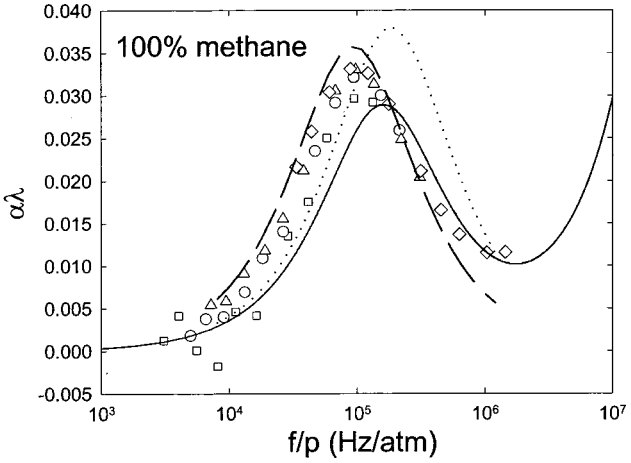

FIG. 8. Results for 100% methane with the Pinkerton diffraction correction at an average temperature of 293.9 K. Data points are for the 92 kHz, 149.1 kHz, 215 kHz, and 1 MHz transducers (squares, circles, triangles, and diamonds, respectively). The solid curve is the calculations based on the vibrational relaxation model of Dain and Lueptow (Ref. 3) summed with the classical attenuation. The dotted curve represents the experimental results from Gravitt *et al.* (Ref. 9), and the dashed curve the results from Edmond and Lamb (Ref. 24).

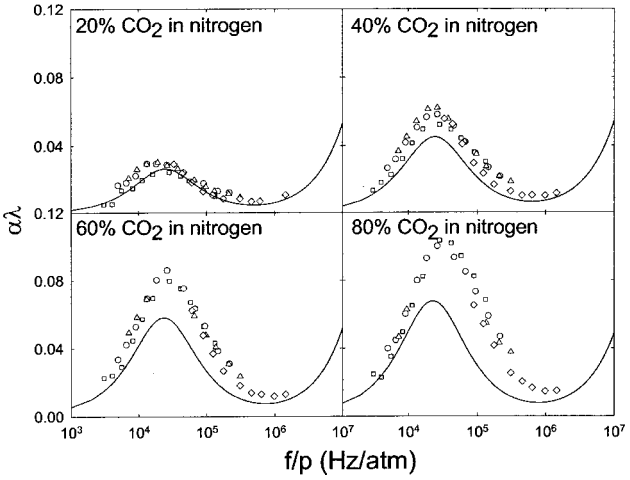

FIG. 10. Results for mixtures of 20%, 40%, 60%, and 80% CO_2 in nitrogen with the Pinkerton diffraction correction at average temperatures of 292.6, 293.7, 293.5, and 294.0 K, respectively. Data points are for the 92 kHz, 149.1 kHz, 215 kHz, and 1 MHz transducers (squares, circles, triangles, and diamonds, respectively). The solid curves are the calculations based on the vibrational relaxation model of Dain and Lueptow (Ref. 3) summed with the classical and diffusional attenuation.

classical attenuation should be the dominant factor with negligible relaxational attenuation in mixtures of oxygen and nitrogen.

C. Methane

The study of methane provides a case where a strong relaxation frequency is present in the range of frequencies measured. The attenuation spectrum for 100% methane is shown in Fig. 8. Again the different transducers agree fairly well. The attenuation for 100% methane has been studied previously. Studies by Edmonds and Lamb[24] and by Gravitt, Whetstone, and Lagemann[9] were carried out using acoustic resonance tubes in a similar frequency range and at similar temperatures. Fits to these measurements are included in Fig. 8 as dashed and dotted curves, respectively. Our measurements agree better with the results of Edmond and Lamb. The variation in attenuation between researchers may result from the sensitivity of attenuation in gases to impurities. In particular small concentrations of water can cause a large shift in the relaxation peak of the attenuation spectrum in other gases.[1,25,26] The calculations of Dain and Lueptow[3] (solid line) agree fairly well with the measurements, although the amplitude of the attenuation peak is slightly lower than the measured peak.

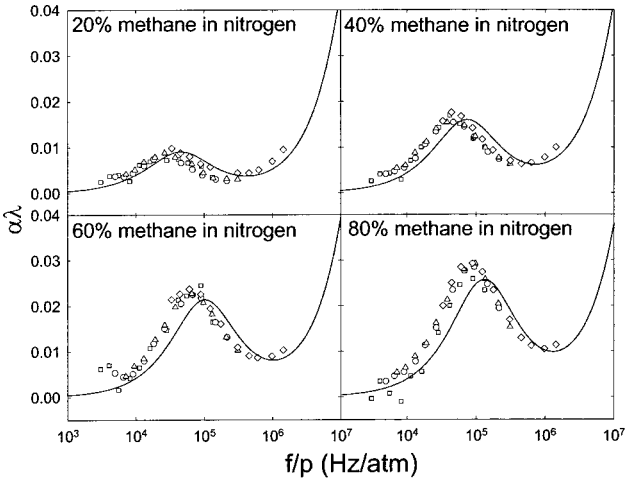

FIG. 9. Results for mixtures of 20%, 40%, 60%, and 80% methane in nitrogen with the Pinkerton diffraction correction at average temperatures of 293.2, 293.0, 293.4, and 295.0 K, respectively. Data points are for the 92 kHz, 149.1 kHz, 215 kHz, and 1 MHz transducers (squares, circles, triangles, and diamonds, respectively). The solid curves are the calculations based on the vibrational relaxation model of Dain and Lueptow (Ref. 3) summed with the classical and diffusional attenuation.

The attenuation spectrum for mixtures of methane and nitrogen are shown in Fig. 9. The results from the different transducers at the same f/p overlap quite well. In addition, the Dain and Lueptow model predicts the attenuation spectrum very accurately. The relaxation peak shifts to a higher frequency and increases in magnitude as the fraction of methane increases. This is related to the increasing dominance of methane relaxation modes as the fraction of methane increases.

D. Carbon dioxide

The attenuation spectra for mixtures of carbon dioxide in nitrogen are shown in Fig. 10. The different transducers again give fairly similar results. Like the relaxation frequency in methane, the amplitude of the peak increases with increasing concentration of carbon dioxide, but the shift in frequency is much smaller than it is for methane/nitrogen mixtures. Also note that the magnitude of the attenuation is substantially larger for carbon dioxide than for methane.

Carbon dioxide has been studied so extensively that it is used in many textbooks as an example of attenuation in a gas.[2] Leonard[27] and Fricke[28] measured the attenuation in pure carbon dioxide at the same frequency and temperature range as the present experiment. Leonard used a pulsed technique to measure the attenuation and found the peak attenu-

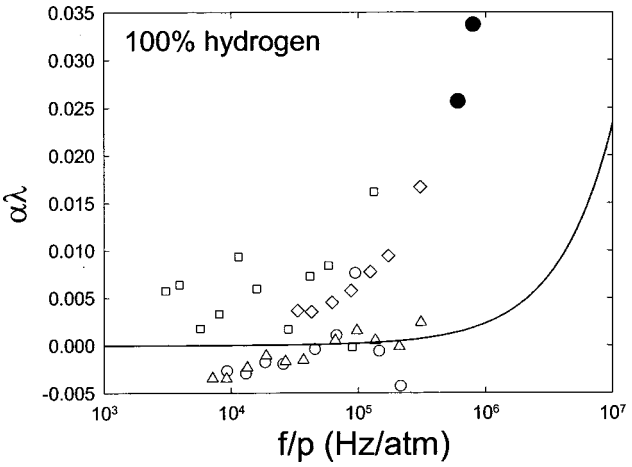

FIG. 11. Results for 100% hydrogen with Pinkerton diffraction correction at an average temperature of 293.8 K. Data points are for the 92 kHz, 149.1 kHz, 215 kHz, and 1 MHz transducers (squares, circles, triangles, and diamonds, respectively). The solid curve is the sum of the classical and diffusional attenuation. The filled circles are data from Winter and Hill (Ref. 30).

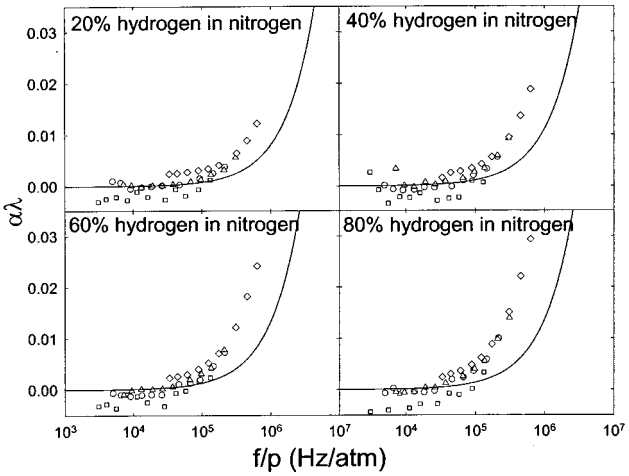

FIG. 12. Results for mixtures of 20%, 40%, 60%, and 80% hydrogen in nitrogen with the Pinkerton diffraction correction at average temperatures of 298.6, 298.2, 297.9, and 297.8 K, respectively. Data points are for the 92 kHz, 149.1 kHz, 215 kHz, and 1 MHz transducers (squares, circles, triangles, and diamonds, respectively). The solid curves are the classical and diffusional attenuation. The vibrational relaxation is negligible.

ation of $\alpha\lambda = 0.125$ at $f/p = 30$ kHz/atm. Fricke measured attenuation in a cubical resonance chamber[29] and found the peak attenuation of $\alpha\lambda = 0.115$ at $f/p = 20$ kHz/atm. For our experiments at 100% carbon dioxide, the attenuation was so strong that the signal arriving at the receiver was too small to be reliably detected even for very small separation distances. However, considering the trend with increasing CO_2 concentration in nitrogen, one could expect 100% CO_2 to have a relaxation peak at a frequency slightly higher than the value of $f/p = 28$ kHz/atm and an amplitude higher than the value of $\alpha\lambda = 0.10$, that we measured for 80% CO_2 in N_2. Furthermore, the slight upward shift in the measured relaxation frequencies and the noticeable increase in the magnitude of the relaxation peaks in Fig. 10 are consistent with previous measurements for small amounts of carbon dioxide in nitrogen.[22]

The calculations for carbon dioxide from our model provide a qualitative representation of the experimental results. The similarity of the frequency for the relaxation peak in the attenuation spectrum with increasing CO_2 concentration is fairly well reproduced. However, the model underestimates the amplitude of the relaxation peak, especially for high CO_2 concentrations. This discrepancy could be the result of the linear structure of the carbon dioxide molecule, which was probably not adequately taken into account in the model for the collisional dynamics.

E. Hydrogen

The acoustic attenuation spectrum for 100% hydrogen is shown in Fig. 11. In this case the values for different transducers do not agree as well as for the other gas mixtures. One problem is that the speed of sound in hydrogen (1306 m/s) is much higher than that in any of the other gases. This results in reflections arriving more quickly at the receiver and being more likely to interfere with the attenuation measurements. More noise may also be present in the system from the excitation of the emitting transducer.

Winter and Hill measured the attenuation in pure hydrogen at high frequencies using a pulse technique.[30] Their results show a large increase in attenuation per wavelength ($\alpha\lambda$) above 1 MHz as indicated by filled circles in Fig. 11. The slight excess energy absorption above the classical case may be related to rotational relaxation in hydrogen with a peak near 20 MHz that affects attenuation above 1 MHz.

Figure 12 shows the attenuation spectrum for mixtures of hydrogen/nitrogen. The scatter observed in the mixtures is similar to that seen for mixtures of oxygen and nitrogen. The calculations for classical attenuation plus the attenuation due to diffusion match the experiments for lower frequencies but fall below the experimental results at high frequencies, especially for higher concentrations of hydrogen. The discrepancy between the calculations and the data is presumably due to the rotational relaxation of hydrogen at high frequencies.

V. CONCLUSIONS

Acoustic attenuation in gases is challenging to measure and predict. Nevertheless, we have been able to measure the attenuation in pure gases and binary gas mixtures. The measurements are in good agreement with previous data. Air and mixtures of oxygen and nitrogen measured using our experimental technique agree well with previous measurements. Our calculations based on the Dain and Lueptow model agree well with experiments for methane and mixtures of methane and nitrogen. In particular, the calculations reproduce the shift in frequency and magnitude of the relaxation peak with increasing methane concentration. Also the calculation for mixtures of carbon dioxide and nitrogen qualitatively agree with the data, showing that the frequency of the relaxation peak in the attenuation spectrum does not shift significantly with increasing CO_2 concentration, while the magnitude does increase. The model also does well in predicting negligible vibrational relaxation for hydrogen. Because the model does not include rotational relaxation, it does not match the measurements for attenuation at higher frequencies in hydrogen. Although the Dain and Lueptow

TABLE II. The collisional diameter (σ), the force constants (ε_{LJ}), the vibrational modes, the degeneracies (g), and the vibrational amplitude coefficients for gases that are necessary for the relaxational attenuation calculations with the Dain and Lueptow model (Ref. 3).

Gas	σ (Å)	ε_{LJ} (cal mol^{-1})	Normal modes of vibration (cm^{-1})	g	Vibrational amplitude coefficients (amu^{-1})
O_2	3.548	175	$v=1554$	1	0.0625
N_2	3.546	159	$v=2331$	1	0.0714
CH_4	3.759	286	$v_1=2915$	1	0.9921
			$v_2=1534$	2	0.9921
			$v_3=3019$	1	0.9923
			$v_4=1306$	3	0.8368
H_2	2.761	75.5	$v=4160$	1	1.0
CO_2	3.99	378	$v_1=1333$	1	0.05
			$v_2=667$	2	0.05
			$v_3=2349$	1	0.05

model should be applicable to gas mixtures of three or more components, further testing is necessary to validate the model in these cases.

ACKNOWLEDGMENTS

This work was supported by NASA, DOE, and the Oklahoma Center for the Advancement of Science and Technology. We thank G. Mozurkewich and B. Ghaffari of Ford Motor Company for helpful discussions.

APPENDIX

Acoustic attenuation in a gaseous medium results from viscous dissipation, irreversible heat conduction, diffusion of gas components, and molecular relaxation. The theoretical curves in this paper are based on appropriate models for each of these phenomena. The total attenuation is the sum of the attenuation due to all three mechanisms, each addressed separately below. All calculations were carried out for a temperature of 292 K and a pressure of 1 atm.

Classical attenuation: The attenuation related to viscous dissipation and irreversible heat conduction are based on the classical formulation by Stokes and Kirchhoff[2] using the shear viscosity, the thermal conductivity, and the specific heats for the gas mixtures calculated according to commercial software.[31]

Diffusional attenuation: The attenuation due to diffusion of the gas components is calculated using Eq. 14.3.19 in Bhatia[2] with the mutual diffusion coefficients from Lide,[32] and neglecting thermal diffusion. For the gas mixtures studied here, attenuation from diffusion is negligible although we have included it in the calculations. An exception occurs in the case of mixtures of hydrogen and nitrogen.

Relaxational attenuation: The theory of relaxational attenuation for vibrational modes of a polyatomic gas mixture is based on the acoustic equations for a plane wave process in a continuous medium accompanied by semimacroscopic population equations for the number of gas molecules in a given energy state.[3] The energy equation in the formulation represents the fluctuation of the total energy of the gas mixture including internal molecular energy states. These equations yield a linear system of ordinary differential equations describing multiple relaxation processes in gas mixtures. The equations, presented for a three-component mixture by Dain and Lueptow,[3] can be easily generalized for the mixtures under consideration in the present paper. We assume that energy exchange occurs between all vibrational modes.

Table II provides collisional diameter (σ), the force constants (ε_{LJ}), the vibrational modes, the degeneracies (g), and the vibrational amplitude coefficients for oxygen, nitrogen, water, methane, hydrogen, and carbon dioxide, that are necessary for the model. The normal modes are expressed using the spectroscopic convention in terms of inverse wavelength.

We assume that at room temperature only one-quantum collisional reactions are possible. The calculation of transition probabilities $P_{0\to0}^{1\to0}(j,k)$ and $P_{0\to1}^{1\to0}(j,k)$ is based on the approximate formulas of transition probabilities for polyatomic gases derived by Tanzcos.[6] The depth of the potential well ε_{LJ} and the vibrational amplitude coefficients are provided in Lambert.[33] The vibrational amplitude coefficients for carbon dioxide were adjusted using known vibration relaxation frequency and experimental attenuation curve for pure CO_2. The adjustable values of the collision diameter in the Lennard-Jones potential related to the gases of interest were obtained by the method outlined by Hirshfelder *et al.*[34] The temperature dependent collision diameter for low energy collisions, σ, was calculated using the kinetic theory formula (Eqs. 8.4–8.5 of Ref. 34) for the gas viscosity data and tabulated values of the kinetic integral.[34] The attenuation due to rotational relaxation was not included, because its contribution is quite similar to the classical contribution at the frequencies considered,[1,35] and except for hydrogen/nitrogen mixtures, it is small in the range of frequencies for which measurements were made.

[1] H. E. Bass, L. C. Sutherland, J. Piercy, and L. Evans, "Absorption of sound by the atmosphere," in *Physical Acoustics*, edited by W. P. Mason (Academic, Orlando, 1984), Vol. XVII, pp. 145–232.
[2] A. B. Bhatia, *Ultrasonic Absorption* (Dover, New York, 1984).
[3] Y. Dain and R. M. Lueptow, "Acoustic attenuation in three-component gas mixtures—Theory," J. Acoust. Soc. Am. **109**, 1955–1964 (2001).
[4] Y. Dain and R. M. Lueptow, "Acoustic attenuation in a three-gas mixture: Results," J. Acoust. Soc. Am. **110**, 2974–2979 (2001).
[5] M. N. Kogan, *Rarefied Gas Dynamics* (Plenum, New York, 1969).
[6] F. Tanzcos, "Calculation of vibrational relaxation times of the chloromethanes," J. Chem. Phys. **25**, 439–447 (1956).
[7] K. F. Herzfeld and T. H. Litovitz, *Absorption and Dispersion of Ultrasonic Waves* (Academic, New York, 1959).

[8] W. Tempest and H. D. Parbrook, ''The absorption of sound in argon, nitrogen and oxygen,'' Acustica **7**, 354–362 (1957).
[9] J. C. Gravitt, C. N. Whetstone, and R. T. Lagemann, ''Thermal relaxation absorption of sound in the deuterated methanes at 26 °C,'' J. Chem. Phys. **44**, 70–72 (1966).
[10] T. G. Winter and G. L. Hill, ''High-temperature ultrasonic measurements of rotational relaxation in hydrogen, deuterium, nitrogen and oxygen,'' J. Acoust. Soc. Am. **42**, 848–858 (1967).
[11] L. B. Evans, ''Vibrational relaxation in moist nitrogen,'' J. Acoust. Soc. Am. **51**, 409–411 (1972).
[12] M. C. Henderson, ''Vibrational relaxation in nitrogen and other gases,'' J. Acoust. Soc. Am. **34**, 349–350 (1962).
[13] H.-J. Bauer and R. Schotter, ''Collision transfer of vibrational energy from nitrogen and methane to the carbon dioxide molecule,'' J. Chem. Phys. **51**, 3261–3270 (1969).
[14] D. Telfair and W. H. Pielemeier, ''An improved apparatus for supersonic velocity and absorption measurements,'' Rev. Sci. Instrum. **13**, 122–126 (1942).
[15] J. Krautkrämer and H. Krautkrämer, *Ultrasonic Testing of Materials* (Springer-Verlag, New York, 1990), pp. 58–92.
[16] J. M. M. Pinkerton, ''On the pulse method of measuring ultrasonic absorption in liquids,'' Proc. Phys. Soc. London **62**, 286–299 (1949).
[17] H. W. Lord, W. S. Gatley, and H. A. Evensen, *Noise Control for Engineering* (Robert E. Krieger Publishing Co., Malabar, FL, 1980), pp. 71–73.
[18] A. S. Khimunin, ''Numerical calculation of the diffraction corrections for the precise measurement of ultrasound absorption,'' Acustica **27**, 173–181 (1972).
[19] A. O. Williams, ''The piston source at high frequencies,'' J. Acoust. Soc. Am. **23**, 1–6 (1951).
[20] P. H. Rogers and A. L. Van Buren, ''An exact expression for the Lommel diffraction correction integral,'' J. Acoust. Soc. Am. **55**, 724–728 (1974).
[21] Y. Dain and R. M. Lueptow, ''Diffraction and attenuation of a tone burst in a mono-relaxing medium,'' J. Acoust. Soc. Am., to appear (2003).
[22] A. J. Zuckerwar and W. A. Griffin, ''Resonant tube for measurement of sound absorption in gases at low frequency/pressure ratios,'' J. Acoust. Soc. Am. **68**, 218–226 (1980).
[23] J. G. Parker and D. N. Ritke, ''Vibrational relaxation times of oxygen at high pressure,'' J. Acoust. Soc. Am. **52**, 1380–1384 (1972).
[24] P. D. Edmonds and J. Lamb, ''Vibrational relaxation times of a number of polyatomic gases derived from measurements of acoustic absorption,'' Proc. Phys. Soc. London **72**, 940–948 (1958).
[25] V. O. Knudsen and E. Fricke, ''The absorption of sound in CO_2, N_2O, COS, and in CS_2, containing added impurities,'' J. Acoust. Soc. Am. **12**, 255–259 (1940).
[26] M. C. Henderson, K. F. Herzfeld, J. Bry, R. Coakley, and G. Carriere, ''Thermal relaxation in nitrogen with wet carbon dioxide as impurity,'' J. Acoust. Soc. Am. **45**, 109–114 (1969).
[27] R. W. Leonard, ''The absorption of sound in carbon dioxide,'' J. Acoust. Soc. Am. **12**, 241–244 (1940).
[28] E. F. Fricke, ''The absorption of sound in five triatomic gases,'' J. Acoust. Soc. Am. **12**, 245–254 (1940).
[29] V. O. Knudsen and E. F. Fricke, ''The absorption of sound in carbon dioxide and other gases,'' J. Acoust. Soc. Am. **10**, 89–97 (1938).
[30] T. G. Winter and G. L. Hill, ''High-temperature ultrasonic measurements of rotational relaxation in hydrogen, deuterium, nitrogen, and oxygen,'' J. Acoust. Soc. Am. **42**, 848–858 (1967).
[31] Physical Property Data Service (PPDS2) for Windows (National Engineering Laboratory, Glasgow, or Technical Database Services, Inc., New York City, 1998).
[32] D. R. Lide, *Handbook of Chemistry and Physics* (CRC Press, New York, 2001), pp. 6–192, 193.
[33] J. D. Lambert, *Vibrational and Rotational Relaxation in Gases* (Clarendon, Oxford, 1977).
[34] J. O. Hirschfelder, C. F. Curtiss, and R. B. Bird, *Molecular Theory of Gases and Liquids* (Wiley, New York, 1954).
[35] G. L. Gooberman, *Ultrasonics: Theory and Application* (Hart Publishing Co., Inc., New York, 1968), pp. 113–138.